Frontiers of Information Technology & Electronic Engineering
www.zju.edu.cn/jzus; engineering.cae.cn; www.springerlink.com
ISSN 2095-9184 (print); ISSN 2095-9230 (online)
E-mail: jzus@zju.edu.cn

Developing a power monitoring and protection system for the junction boxes of an experimental seafloor observatory network*

Jun WANG†, De-jun LI†‡, Can-jun YANG, Zhi-feng ZHANG, Bo JIN, Yan-hu CHEN

(*State Key Laboratory of Fluid Power and Mechatronic Systems, Zhejiang University, Hangzhou 310027, China*)

†E-mail: rongjie5257@163.com; li_dejun@zju.edu.cn

Received Mar. 26, 2015; Revision accepted Aug. 10, 2015; Crosschecked Nov. 6, 2015

Abstract: A power monitoring and protection system based on an embedded processor was designed for the junction boxes (JBs) of an experimental seafloor observatory network in China. The system exhibits high reliability, fast response, and high real-time performance. A two-step power management method which uses metal-oxide-semiconductor field-effect transistors (MOSFETs) and a mechanical contactor in series was adopted to generate a reliable power switch, to limit surge currents and to facilitate automatic protection. Grounding fault diagnosis and environmental monitoring were conducted by designing a grounding fault detection circuit and by using selected sensors, respectively. The data collected from the JBs must be time-stamped for analysis and for correlation with other events and data. A highly precise system time, which is necessary for synchronizing the times within and across nodes, was generated through the IEEE 1588 (precision clock synchronization protocol for networked measurement and control systems) time synchronization method. In this method, time packets were exchanged between the grandmaster clock at the shore station and the slave clock module of the system. All the sections were verified individually in the laboratory prior to a sea trial. Finally, a subsystem for power monitoring and protection was integrated into the complete node system, installed in a frame, and deployed in the South China Sea. Results of the laboratory and sea trial experiments demonstrated that the developed system was effective, stable, reliable, and suitable for continuous deep-sea operation.

Key words: Power monitoring and protection, Embedded processor, Seafloor observatory network, IEEE 1588, Junction boxes
doi:10.1631/FITEE.1500099 **Document code:** A **CLC number:** TP202

1 Introduction

Oceans play a decisive role in global climate change, ecological cycles, and species breeding, among others. Seas also contain abundant mineral and biological resources. Thus, marine observation is of great significance to humans for comprehending oceans, exploring biogenesis, maintaining the benign development of ecosystems, predicting natural disasters, and exploring natural resources. With the recent developments in marine science and technology, conventional non-real-time, short-term, and intermittent observations made through off-line devices can no longer satisfy human requirements. Seafloor observatory networks have increasingly attracted attention and have developed rapidly because of their advantages in terms of providing real-time, long-term, and continuous observation data (Dewey and Tunnicliffe, 2003; Chave *et al.*, 2004; Hsu *et al.*, 2007; Barnes and Tunnicliffe, 2008; Kawaguchi *et al.*, 2008; Aguzzi *et al.*, 2011). The Experimental Seafloor Observatory Network System deployed in the South China Sea represents the first attempt to build a regional cabled observatory network in China. In this system, various underwater instruments are connected to junction boxes (JBs). JBs are wired to a

‡ Corresponding author
* Project supported by the National High-Tech R&D Program (863 Program) of China (Nos. 2012AA09A408 and 2012AA09A402), the National Natural Science Foundation of China (No. 51409229), and the Zhejiang Provincial Natural Science Foundation of China (No. LQ14E070002)
ORCID: Jun WANG, http://orcid.org/0000-0002-3291-7214

shore station (SS) via subsea optical-electrical cables which are used to transmit high-voltage power and high-bandwidth communication from the SS to subsea equipment (Chen *et al.*, 2012; Li *et al.*, 2015).

As an indispensable component of underwater observatory network systems, JBs function as intermediate processing nodes between underwater science instruments (SIs) and an SS in power transmission and communication. The motility, stability, and reliability of JBs are crucial to the long-term and reliable operation of an entire seafloor observatory network in extreme deep-sea environments (Woodroffe *et al.*, 2008; Yu *et al.*, 2011). A single failure may cause the entire system to malfunction, and JBs are costly to repair or replace. Therefore, a power monitoring and protection system, which is based on an embedded processor and combined with peripheral circuits, is proposed in the current study according to the actual requirements of a seafloor observatory network and the design principles of industrial products. The primary design objectives are to address power allocation, surge current limitation, real-time monitoring, grounding fault detection, accurate time synchronization, and automated response to the failure of either secondary JBs (SJBs) or terminal SIs. Furthermore, a redundant design is implemented to improve the reliability of the system with the goal of prolonging the system's lifetime.

2 An overview of the seafloor observatory network and the power monitoring and protection system

Fig. 1 shows the structure of the seafloor observatory network and the proposed power monitoring and protection system. The network system consists of an SS, several JBs and branching units, various SIs, and submarine transmission cables. The power feeding equipment (PFE) is linked to a terrestrial power grid and supplies power to the system. Real-time data collected by JBs and by many other types of sensors deployed on the seabed are processed, managed, stored, and maintained by a data management system (DMS), which is connected to the global Internet via a router (Pirenne and Guillemot, 2009; Chen *et al.*, 2013). The IEEE 1588 grandmaster clock provides a microsecond-level accurate timing service to the observatory system when its local time is adopted as the reference; this process is initiated once the clock is synchronized with the Coordinated Universal Time (UTC) by receiving navigation satellite timing signals (del Río *et al.*, 2012; Li *et al.*, 2013). A subsea optical-electrical composite cable is laid on or buried in the seafloor; this cable runs from the SS to the primary JBs (PJBs). High-voltage power and high-bandwidth communication are then transmitted to subsea equipment through the cable. Standard wet-mate connectors are used to connect the JBs to the SIs; these connectors are operated by a remotely controlled underwater vehicle.

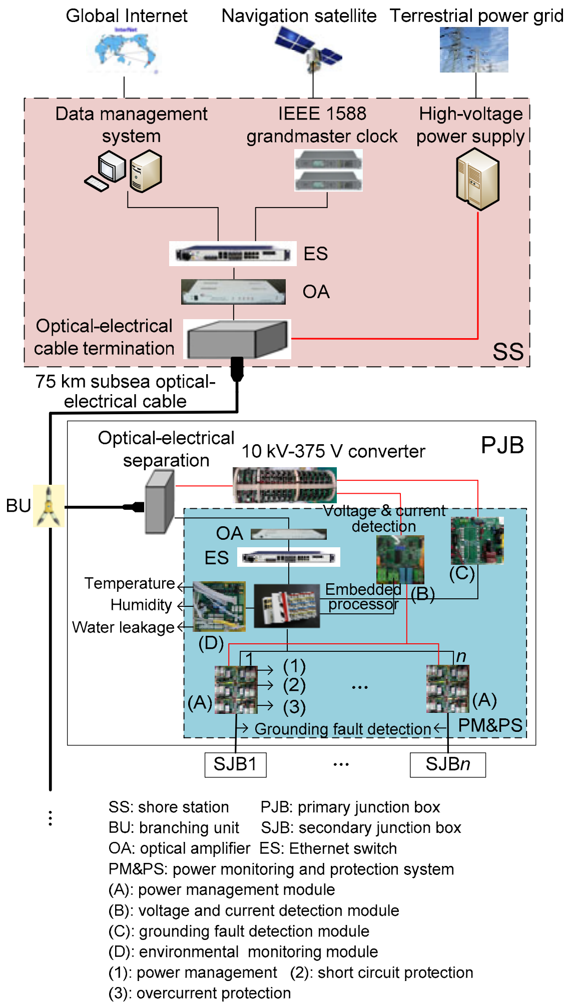

Fig. 1 Tree structure of the seafloor observatory network and the power monitoring and protection system

The requirements for the controller include high reliability and excellent interference resistance capability given the high voltage inside the cavity. A small controller installation space is preferred, and the controller must contain as many analog and digital input and output ports as possible. An embedded processor (CX5010-0111, Beckhoff Automation GmbH & Co. KG, Germany) is selected as the control core of the power monitoring and protection system. Peripheral circuit modules with multiple functions are connected to this processor, which exhibits the characteristics of an industrial personal computer and a programmable logic controller. The processor also has the advantages of reliable control, simple wiring, high stability, long life, compact structure, versatility, and low cost. Furthermore, CX5010-0111 features a built-in capacitive 1-s uninterrupted power supply (UPS) that ensures the safe storage of persistent application data on a CompactFlash card in case of power outages. A maximum of 1 MB of data can be saved, and the UPS can be switched on and off via the basic input/output system (Ioannides, 2004). The basic monitoring elements of the system include output voltages and currents, environmental signals (such as temperature, humidity, and water leakage inside the cavity), and the grounding status of output power. The basic control units of the system include the power switch and measured grounding resistance values. Voltage, current signals, and environmental signals inside the chamber are detected by designing the corresponding sensing and detecting circuits that can collect, process, and output signals. The sample period is 10 ms. The system packages and uploads sample data per second to the monitor server at the SS. The embedded processor samples the collected data cyclically and compares them with the thresholds. If one signal exceeds its threshold beyond the scheduled time, the system implements protective actions, sends warnings to the SS, and records information. Furthermore, the embedded processor synchronizes the time of the built-in IEEE 1588 slave clock module with that of the grandmaster clock for timing accuracy.

The power monitoring and protection system is designed with reference to existing systems, such as the Monterey Accelerated Research System, Victoria Experimental Network Under the Sea, and North East Pacific Time-Series Undersea Networked Experiments, particularly with respect to the system framework and the relay control method (Howe *et al.*, 2006; Chan, 2007). The proposed system differs from existing systems in the following ways: (1) An industrial embedded controller is used in the proposed system to achieve strong anti-interference capability and high reliability. The controller has its own time synchronization module, which can output pulse per second (PPS) time signals with microsecond-level timing accuracy. Therefore, the time synchronization system does not need to configure an additional slave clock. Consequently, cost is reduced and the assembly space is compressed. (2) The methods of limiting the activated surge current vary among different systems. In the proposed system, the surge current is suppressed by positioning the power resistor and mechanical contactor in parallel through a simple and reliable process. (3) The design methods of the software used differ between the proposed system and existing systems. SIMATIC Windows Control Center (WinCC) configuration software is selected and applied to the shore-side computer of the system. This software is open, flexible, and has a user-friendly man-machine interface.

The following challenges are encountered during system development because of the special working environment and requirements: (1) Effective and reliable power management is difficult to achieve because the deep-sea environment is complex and dynamic. Thus, short circuits and overcurrent failures, which require fast and steady automatic responses, may occur frequently. (2) Grounding faults are frequently detected in seafloor observatory networks. Hence, precise and reliable grounding fault detection is the premise and foundation for the normal operation of an observatory system. (3) Times are difficult to synchronize accurately. Several methods are introduced and experimentally evaluated in the subsequent section to solve the aforementioned problems.

3 Methods

3.1 Power management method

The power for the terminal SIs is supplied by the JBs. Power activation and deactivation, monitoring, the limitation of turned-on surge currents, and automatic responses to faults are achieved mainly through the power management method. The traditional control method which adopts only mechanical relay is unsuitable because of the highly technical system indicators including high reliability, a small transient impulse voltage, and fast response. For instance, the switch must be turned off within tens of microseconds in the event of a short circuit. The power management method applied in the proposed system uses a pair of parallel metal-oxide-semiconductor field-effect transistors (MOSFETs) and a mechanical contactor in series. Fig. 2 depicts the structure of the power management module with an output of 375/48 V. When the system is turned on, the mechanical contactor is normally closed at first; then the MOSFETs are activated after 500 ms to ensure continuous power supply. When the system is turned off, the MOSFETs are normally deactivated and the mechanical contactor is opened after 500 ms to cut off the power supply. The driving circuit of the MOSFETs can initiate hardware shutdown within tens of microseconds by using the built-in inspection module in case of a short circuit. The overcurrent signal sent by the overcurrent detection chip enters the driving circuit of the MOSFETs and switches off the MOSFETs in the event of an overcurrent.

The MOSFETs and mechanical contactor perform different functions. The former can realize rapid on-off switching and inhibit or alleviate the damage to the contactor and to the terminal loads caused by voltage surge. This surge is the result of mechanical jitters which occur during the switching moment of the mechanical contactor. The contactor can facilitate complete galvanic isolation between the lower and upper circuits; it is placed near the output terminal to ensure reliable load isolation in case of a fault. The redundancy design method is adopted to enhance the reliability of the power monitoring and protection system and to guarantee a long normal operating state. The parallel mode is used for the dual MOSFETs, and the working currents of the MOSFETs are halved to prolong their service life.

Upon system activation, the surge current is limited by incorporating a surge-suppressing circuit in series with the power supply line. This circuit consists of a 100 Ω/100 W power resistor and a mechanical contactor in parallel. When the system is turned on, the mechanical contactor of the circuit is opened and the current forms a loop that passes through the power resistor. Surge current energy is then absorbed by the power resistor, thus limiting the surge current. The control circuit of the contactor is fully charged within hundreds of milliseconds after the switch is closed. The contactor is then switched on to short out the power resistor. The final current loop of the power supply circuit is formed through the contactor.

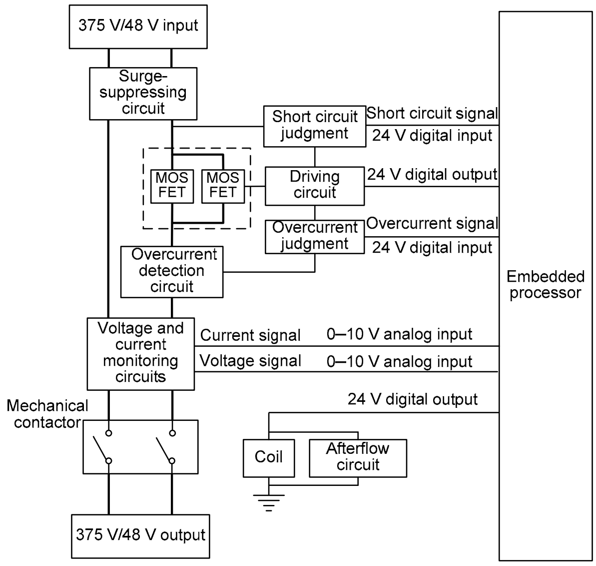

Fig. 2 Structure of the power management module

3.2 Grounding fault detection method

A pair of power supply lines of the JBs that provide 375/48 V power is suspended over the seawater ground. Grounding faults occur when a single wire comes into contact with seawater or with the cavity of the JBs, as well as when the relative impedance between the wire and seawater is too small. The insulation performance of the power supply lines degrades with the operating time of the JBs in an extreme submarine environment. The internal parts of underwater SIs may also be exposed upon contact with seawater or with a reduction in impedance, which easily initiates grounding faults. Single-wire grounding does not induce a short circuit or a large current leakage because the positive and negative terminals of the power supply lines do not come into contact with each other. Moreover, power supply ports do not form a loop through seawater; thus, the system continues to operate normally. By contrast, unipolar grounding significantly increases the risk of a short circuit and affects the measurement accuracy of the system. Furthermore, the fault current causes electrochemical corrosion and damages the connectors of the cables. Therefore, detecting grounding faults in each power supply line is critical (Lu, 2006).

The grounding fault detection module is shown in Fig. 3. $G-$ and $G+$ are the command signals of negative and positive grounding fault detection, respectively; these signals are followed in turning switches S_1 and S_2 on and off, respectively. R_f is the resistance value between the power supply lines of the JBs and seawater ground. Power supply line+, R_1, R_3, R_f, and power supply line− form a current loop when S_1 is closed. Thus, the loop current can be determined, and the grounding resistance value R_f between power supply line− and seawater ground can be calculated by determining the voltage value of R_3. Power supply line−, R_2, R_3, R_f, and power supply line+ form another current loop when S_2 is closed. This condition indicates that the grounding resistance value R_f between power supply line+ and seawater ground can be calculated by detecting the voltage value of R_3 in the same manner. This voltage value is amplified and filtered by an operational amplifier after the voltage passes through an isolation amplifier. Then the processed voltage signal is input into the embedded processor to calculate grounding impedance. When the R_f value is less than the given threshold (200 kΩ), a grounding fault is likely to be initiated.

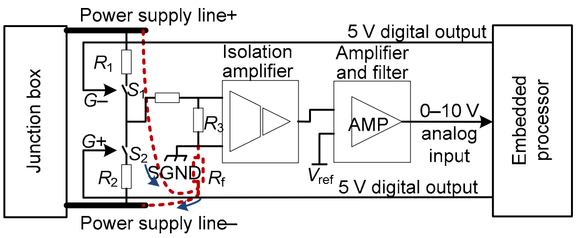

Fig. 3 Structure of the grounding fault detection module

3.3 Time synchronization method

Time synchronization is a significant function in a seafloor observatory network. The time-series data collected from different underwater sensors at various sites, which may be located from a few meters to thousands of kilometers away, must be time-stamped for accurate analysis. The JBs operate steadily by monitoring and controlling external loads and internal environmental variables. The real-time performances of these signals should be identified to determine the conditions of the JBs. The series of data acquired by the system must share a common time reference with all the instruments and sensors, which suggests that time stamps should follow a recognized time reference. Low-accuracy time units, such as second or millisecond, are adequate for some observations; for other observations, such as seismic detection and acoustic communication, precise time units of up to microsecond are preferred (Milevsky and Walrod, 2008; Lentz and Lécroart, 2009).

The IEEE 1588 standard is applied in the current study to provide time with microsecond accuracy. This standard specifies the precision time protocol (PTP) and facilitates robust, highly accurate, and cost-effective time synchronization. PTP measures clock skewness and network delay between a grandmaster clock and slave clocks mainly through four types of time messages that are exchanged across a network: Sync, Follow_Up, Delay_Req, and Delay_Resp. The message transmission process is depicted in Fig. 4. PTP time synchronization is implemented in two steps: the measurement of master-slave clock offset and the measurement of network delay (Li *et al.*, 2013).

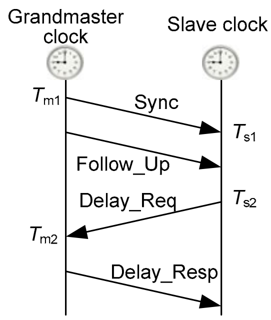

Fig. 4 Synchronization principle of PTP

The measurement process of master-slave clock time deviation is described as follows.

The grandmaster clock sends a Sync message to a slave clock and records the accurate time of transmission as T_{m1}. The slave clock receives this message and records the accurate time of reception as T_{s1}. Then the grandmaster clock sends a second message called Follow_Up, which contains the time stamp T_{m1}, to the slave clock. Assuming that the network delay between the grandmaster and slave clocks

(T_{delay}) is known, the time deviation between the grandmaster and slave clocks (T_{offset}) can be calculated as follows:

$$T_{offset} = T_{s1} - T_{m1} - T_{delay}. \quad (1)$$

The master-slave clock network delay measurement process is explained as follows.

The slave clock sends a Delay_Req message to the grandmaster clock and records the accurate time of transmission as T_{s2}. The grandmaster clock receives the message and marks the accurate time of reception as T_{m2}. Then the grandmaster clock sends a Delay_Resp message, which contains the time stamp T_{m2}, to the slave clock. The network delay (T_{delay}) can be calculated as

$$T_{delay} = T_{m2} - T_{s2} + T_{offset}. \quad (2)$$

By combining and solving Eqs. (1) and (2), we can obtain

$$T_{delay} = \frac{(T_{m2} - T_{s2}) + (T_{s1} - T_{m1})}{2}, \quad (3)$$

$$T_{offset} = \frac{(T_{s1} - T_{m1}) - (T_{m2} - T_{s2})}{2}. \quad (4)$$

3.4 General variable monitoring method

Current and voltage detections facilitate the direct judgment of system failures, such as overcurrents and short circuits. These detection processes are closely related to the automatic protection and intelligent control of a system; they are also the most important among all analog detection processes. The procedures require mainly real-time and accurate measurements. Considering the application conditions and actual requirements of the system, a detection module, which consists of an electrical isolation sensor and peripheral circuits with properties that include small size, high accuracy, high isolation, low drift, and low power consumption, is designed and manufactured. The measurement accuracy of this detection module can reach an accuracy level of 0.1%, and its input frequency response ranges from 0.02 Hz to 10 kHz. In voltage detection, a special high-precision divider resistance is adopted to divide voltage accurately. In current detection, a highly accurate constantan resistance is used to convert a current signal directly into a voltage signal within a particular input range. The detection of internal environmental signals, such as temperature, humidity, and water leakage, plays an auxiliary role in understanding the real-time operating status of a system. The accuracy requirements for such detection processes are relatively low, and temperature and humidity can be monitored using off-the-shelf sensors. Water leakage can be detected with a leakage-sensing wire, which is composed of a fluoropolymer material and produced through conductive polymerization technology. The resistance between two parallel sensing wires, which are installed at both ends of the cavity, changes in the event of a leakage because of the partial short circuit caused by seawater.

3.5 Software design method

Communication between the embedded processor, which serves as the node controller of the system and the port modules, is transmitted via an industrial Ethernet protocol called Ethernet control automation technology (EtherCAT). This technology was studied and developed by Beckhoff Automation GmbH & Co. KG (Germany); it ensures fast, real-time data acquisition and interaction. The software of the node controller is written in structured text language in combination with a ladder diagram (Qi *et al.*, 2010; Cena *et al.*, 2012), and the main functions of this controller include the following aspects: (1) main program scanning—collecting system monitoring data, processing abnormal data, executing instructions from the DMS (function as the shore-side computer of the system), and troubleshooting; (2) data communication—facilitating remote data communication between the shore-side computer and the node controllers; (3) time synchronization—synchronizing times with the PTP grandmaster clock, obtaining synchronized times with microsecond-level accuracy and converting them into 64-bit systematic times for the embedded processor, and triggering the output of PPS signals. A shielded wire is used to block electromagnetic interference caused by the varying electric fields inside the cavity. Consequently, the processes of relevant data collection and instruction transmission between peripheral circuits and the embedded processor can be robust. Fig. 5 presents the control flowchart of the node controller software for the proposed system.

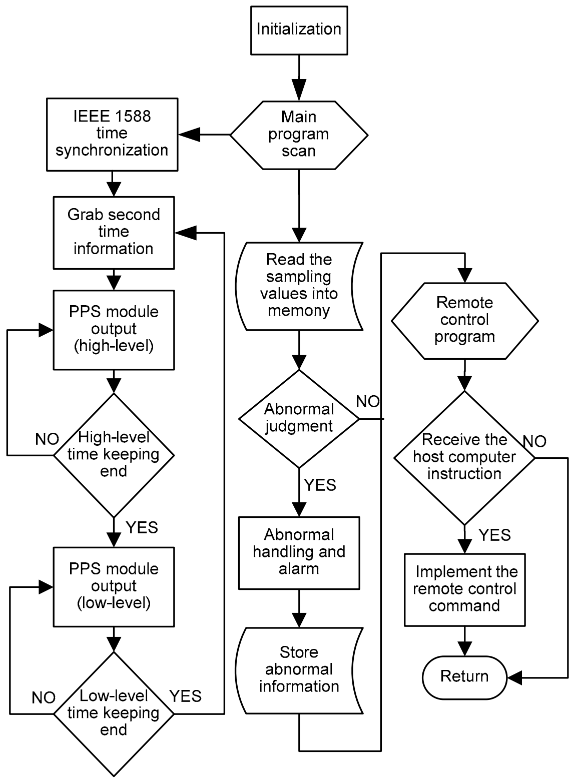

Fig. 5 Control flowchart of the node controller software

The shore-side computer software, which performs power monitoring and protection functions based on the embedded processor, must be designed to satisfy the following aspects: (1) with a user-friendly and convenient human-computer interactive interface; (2) with high expandability; (3) with real-time display, transmission, and data storage; (4) with a failure alarm and filing system; (5) with remote monitoring and control. Given the aforementioned requirements, SIMATIC WinCC (Siemens AG, Germany) is selected as the programming and human-computer interface environment of the shore-side computer of the system due to the openness and flexibility of this software (Sun *et al.*, 2011).

4 Experimental verification

A prototype of the power monitoring and protection system was built in laboratory, and a comprehensive functional verification of this system was conducted to ensure its effectiveness and reliability prior to deployment on the seabed. Several off-the-shelf devices, such as the grandmaster clock, were used in the experimental verification process, and some devices were customized, including the PFE which converts a three-phase alternating current (AC) into 10 kV direct current (DC) and has a maximum output of 10 kV/10 kW, the high-voltage power converter that converts 10 kV DC to 375 V DC, and the DMS. The equipment, as well as the power monitoring and protection system, was assembled into a cabled observatory network system in the laboratory, as shown in Fig. 6.

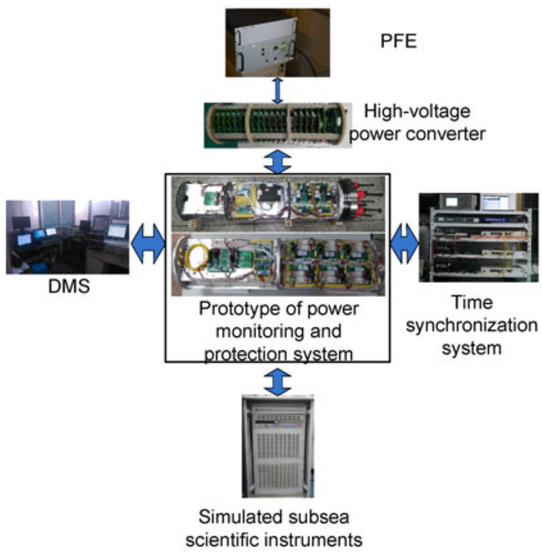

Fig. 6 Prototype of a cabled observatory network system in a laboratory

4.1 Power management and protection against short circuiting and overcurrents

Reliable power management is a key technology in the system. The power management module, which consists of MOSFETs and a contactor, is adopted in this system based on the preceding description. The switching action sequence of the MOSFETs and the contactor is critical; a correct switching order not only provides stable power to the system but also protects the MOSFETs and the contactor, in addition to improving system reliability and service life. An incorrect sequence results in an output voltage with a significant surge, which endangers the power management module.

A test was conducted using a digital oscilloscope to measure the related voltages when the switch was turned on and off. The results are shown in Fig. 7. To demonstrate the successive action sequence of the contactor and the MOSFETs intuitively under this condition, Ch1 measurement indicates the voltage between the front end of the MOSFETs and the negative terminal at the back end of the contactor. Ch2 measurement indicates the voltage between the positive and negative terminals at the back end of the contactor. The voltage of Ch1 first increases to 375 V; subsequently, the voltage of Ch2 reaches the same value after a time delay of 500 ms when an instruction is sent for activation, as indicated in Fig. 7a (The maximum pickup and release times of the mechanical contactor are 25 and 8 ms, respectively. To avoid mutual interference in the switching actions between the contactor and MOSFETs and to maintain an adequate time margin, a time interval of 500 ms was set). Fig. 7b depicts the opposite situation; i.e., an instruction is sent for deactivation. In this case, the voltage of Ch2 first decreases to 0 V; then the contactor is turned off after 500 ms, after the switch is deactivated. All the aforementioned practical action sequences (activation and deactivation) agree with those of the theoretical design (A ground fault is detected in the high-voltage probe of the oscilloscope that is connected to Ch1; interference with 50-Hz frequency was introduced into the measurement, and the oscillations displayed in the figures do not affect the test results).

The deep-sea environment is complex and dynamic. Any connection node or cable may fail during seafloor observatory network operation. On the one hand, improving the reliability and reducing the failure probability of the system through a redundancy design are necessary. On the other hand, the system should be capable of diagnosing failure and acting within a remarkably short time period once the system fails to avoid damaging the other nodes and cables, as well as to minimize the risk of danger.

Fig. 8 shows the automatic control response curves of the power management module in the event of failure. Fig. 8a depicts the response curves during a short circuit, where Ch1 indicates the output current, Ch2 the output voltage, and Ch3 the

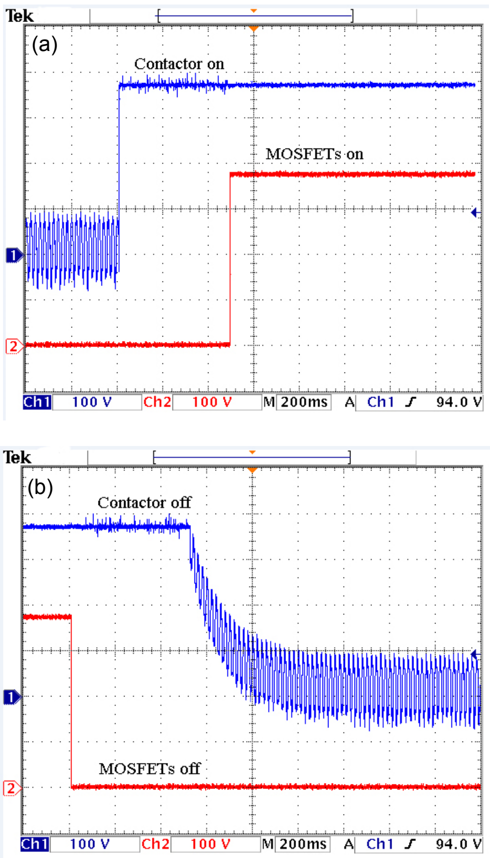

Fig. 7 Results of the action sequence when turning the switch on (a) and off (b)

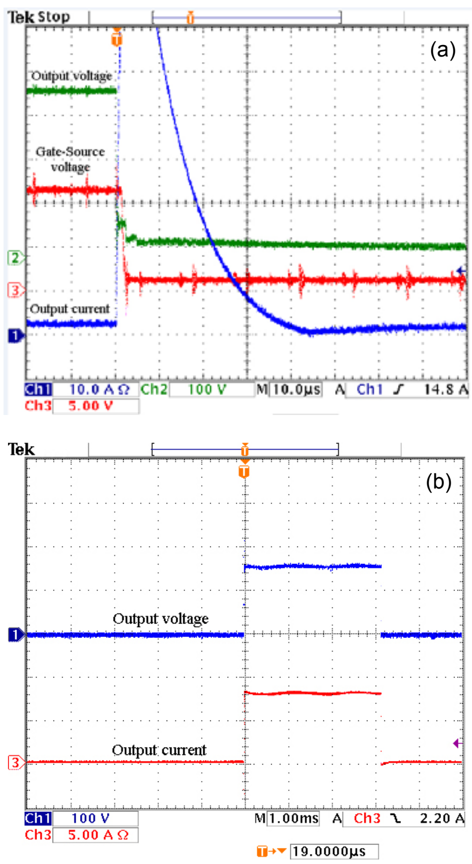

Fig. 8 Curves of short-circuit protection (a) and over-current protection (b)

gate-source voltage (V_{GSS}) of the MOSFETs. The chart shows that the output current increases to >70 A when short circuit occurs at the load terminal. In this event, the driving circuit of the MOSFETs detects the short-circuit signal and immediately initiates hardware shutdown. The driving voltage of the MOSFETs (V_{GSS}) is reduced from +12 V to a low level (0 V) within 5 μs, and the overall output is cut off. Moreover, the output current decreases to a safe value within 40 μs, which protects against short circuits. Fig. 8b illustrates the response curves during overcurrents. Ch1 indicates the output voltage and Ch3 the output current. An overcurrent detection circuit, which consists of a functional chip and relevant peripheral circuits, detects overcurrents and protects against them. When the chip detects a large current (>7 A) that lasts more than 3 ms, the chip sends out a signal to the driving circuit of the MOSFETs and turns off these transistors. The switching sequences and fault automatic responses observed at an output of 48 V are similar to those determined at 375 V. The maximum working voltage of the contactor during activation and deactivation is 1200 V DC, and the maximum carrying current is 50 A. The drain-source voltage (VDSS) of the MOSFET is 600 V, the continuous drain currents (ID) are 47 A and 29.7 A at 25 °C and 100 °C, respectively, and the gate-source voltage (VGSS) is ±30 V. The maximum steady-state current for the 400 V and 48 V ports are 5 A and 4.2 A, respectively. A slight dead short can be fed within a few microseconds, and the high-voltage power supply is unaffected in the event of an overcurrent or a short circuit because of the fast automatic response of the power management module.

4.2 Grounding fault detection

Grounding faults are difficult to reproduce in a laboratory. Thus, a precision potentiometer was connected to simulate actual grounding resistance from 0 to 10 MΩ between seawater ground and the positive or negative power supply line. The output responses of the circuit were detected, and the measured values were calculated. Fig. 9 displays the actual resistance values of the potentiometer, the calculated grounding resistance values, and the fault currents under different output voltages. The actual resistance values of the potentiometer coincide well with the calculated grounding resistance values, and the errors are within 2%. The designed grounding fault detection method thus performs the expected detection function.

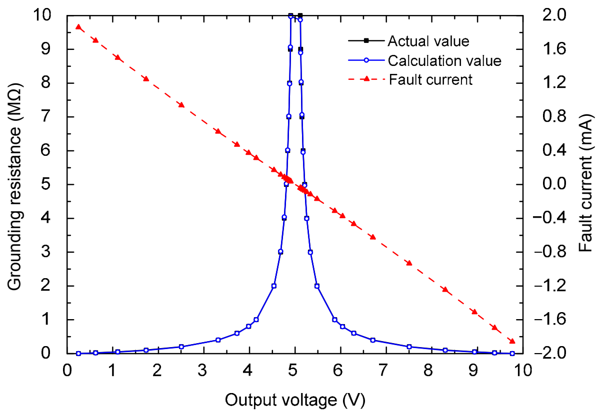

Fig. 9 Curves of the grounding resistance and fault current under different voltages

4.3 Time synchronization

The embedded processor installed inside the JBs achieves IEEE 1588 microsecond-level time synchronization with the PTP grandmaster clock installed at the SS through Ethernet. In addition, the processor provides highly accurate PPS timing signals for the JBs and the terminal SIs. The laboratory test scheme for the time synchronization function is shown in Fig. 10a. The PTP grandmaster clock synchronizes its local time with UTC by receiving Global Positioning System (GPS) or BeiDou satellite timing signals through either a GPS antenna or a BeiDou antenna and module. Then the PTP grandmaster clock applies its local time as the time reference to provide a timing service for the PTP slave module; this module is connected to the embedded processor via the EtherCAT interface and through Ethernet switches that support the IEEE 1588 protocol. The PPS output module is a two-channel digital output module with a time stamp function. The delay of the internal output circuit is within 10 ns, and the two channels of the PPS signals can be output after the PTP slave clock module is synchronized through programming. If additional PPS signals are required, a PPS frequency distribution amplifier can be used; this amplifier can expand one PPS signal into multiple PPS signals while maintaining accuracy and voltage level (Han and Jeong, 2010; Ouellette *et al.*, 2011).

The time synchronization cycle between the grandmaster clock and the slave clock was set to 1 s. The PPS signals output by the PTP grandmaster clock and the two channels of the PPS output module were accessed by Ch1, Ch2, and Ch3 of the oscilloscope, respectively. The signals were measured continuously for 24 h and the results are exhibited in Figs. 10b and 10c. The charts suggest that the increasing edge deviation of the signals output by the PTP grandmaster clock and by the PPS output module ranges in −20–200 ns. The mean time deviation between the grandmaster clock and slave clock module is 78.6 ns, and the standard deviation is 39.5 ns. The mean offset was attributed to the asymmetrical background traffic on the communication link in the measurement. The experimental results prove that the designed time synchronization method can provide a timing service with microsecond accuracy to the system.

4.4 Software testing

Functional pool testing was conducted continuously for 120 h in the laboratory to verify the operation of the shore-side computer software for the power monitoring and protection system. The software interface during system operation is shown in Fig. 11. The underwater system can receive the correct control signals sent by the host computer by running this software. Each output can be monitored and controlled through the interface in real time. Meanwhile, the internal environmental signals of the cavity were surveyed, and the expected functional targets were achieved.

The script of the shore-side computer software, which runs in the background, writes the collected data sent by the subsea system into the local file (in TXT format) at a rate of once per second. Fig. 12 depicts the voltage and current monitoring data of one output channel in tank testing for 24 h. The output was turned on and off several times within this period, and the output response of the voltage is consistent with the current illustrated in the diagram. The output voltage is stable, whereas the output current fluctuates because the connected load is an SJB that randomly powers its loads by activation and deactivation.

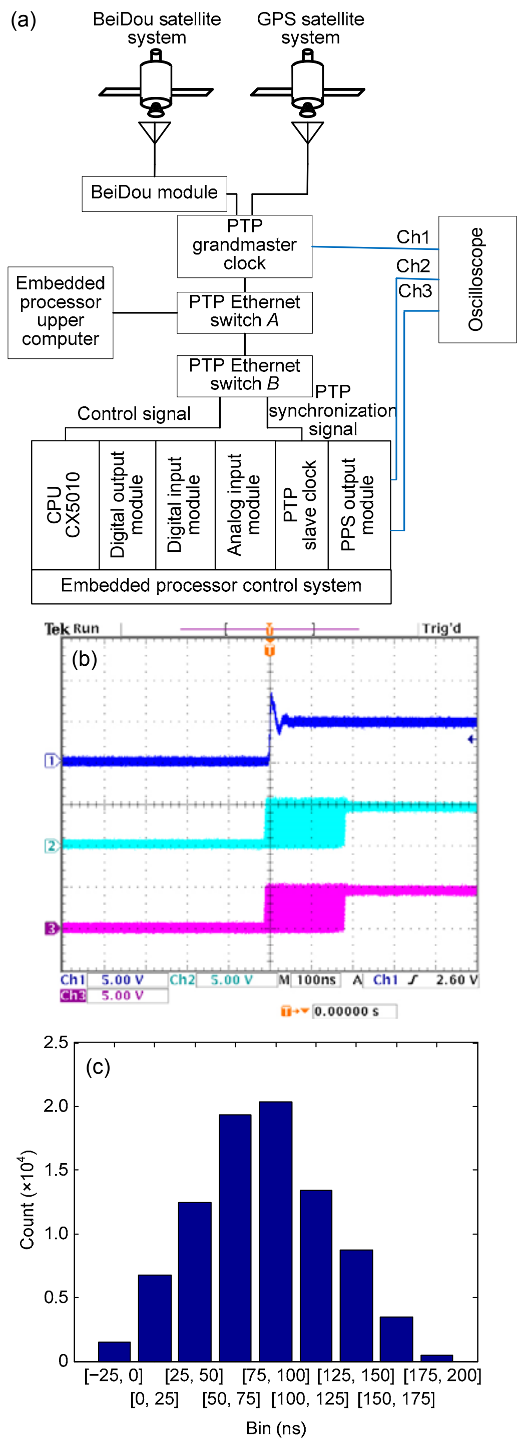

Fig. 10 Laboratory test scheme of the time synchronization function (a), results of long-term PPS signals (b), and PPS signal delay histogram (c)

4.5 Sea trial

To test the ultimate application of the system on the seafloor, a sea trial was successfully conducted in

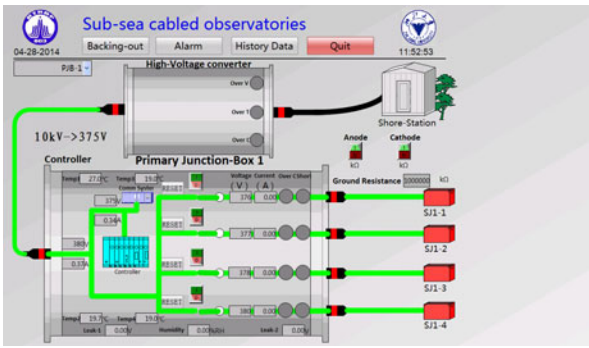

Fig. 11 Software interface during system operation

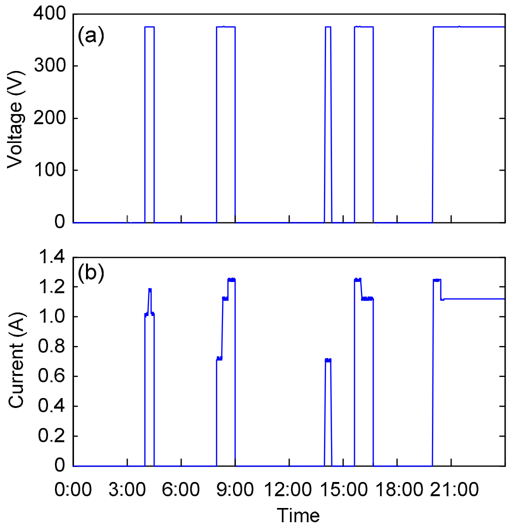

Fig. 12 Voltage (a) and current (b) monitoring data of one output channel for 24 h

the South China Sea in Aug. 2013 (Fig. 13). The system was packaged in a frame and deployed on the seabed at a depth of approximately 200 m. High-voltage power and high-bandwidth communication were normally transmitted to the system through a 75-km optical-electrical cable from the SS located near the beach with the aid of available power and global Internet. The power monitoring and protection system worked properly and stably for the first 30 min after startup. The detected voltages and currents, and the various environmental parameters inside the cavity, were normal during system operation; each output port could be turned on and off by sending instructions from the shore-side computer. However, the JBs were invalidated after 30 min because the dry-mate connector between the high-voltage power converter cavity and the primary control cavity broke down. Furthermore, both the positive and negative 375-V power supply lines were shorted by the seawater. Thus, the system was recycled. Despite the short operating period of the JBs before failure, the sea trial represents the first attempt to build a regional cabled observatory network in China and establishes a good foundation for the final deployment of the system in the summer of 2015.

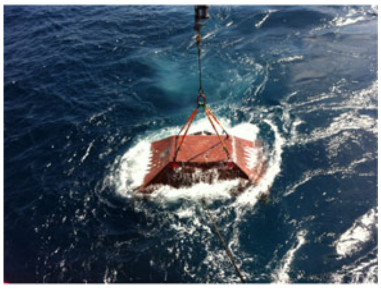

Fig. 13 Deployment of the experimental assembly system

5 Conclusions

A power monitoring and protection system was proposed and constructed in this study to facilitate power monitoring and management. This system also enables real-time surveying of the environmental variables of JBs, grounding fault detection, and accurate time synchronization for the entire system according to the specific condition of the seafloor observatory network, the working environment, and the functional requirements of JBs. This article has reported each section of the system, i.e., power management, grounding fault detection, time synchronization, general monitoring, and software design. A two-step power management module which consists of MOSFETs and a mechanical contactor was adopted for power management. Moreover, a new circuit structure was designed to detect the grounding resistance of a single power supply line with respect to the sea ground. An effective time synchronization method that uses the IEEE 1588 protocol was applied to facilitate microsecond-level time precision in the system. The system software developed in the WinCC environment exhibited powerful functions and an intuitive and user-friendly interface. The EtherCAT bus demonstrated high-speed, real-time operation, and favorable expandability advantages. Prior to deployment on the seabed, each section of the system was tested in the laboratory to ensure effective functionality and high reliability. Finally, a sea trial was conducted in the South China

Sea. The developed system exhibited reliable power management and general monitoring, exact grounding fault detection, and accurate time synchronization. Although the system was successfully validated in terms of functional aspects, further investigation must be conducted to ensure its long-term operation and reliability. The applied system will be deployed later in 2015.

References

Aguzzi, J., Mànuel, A., Condal, F., *et al.*, 2011. The new seafloor observatory (OBSEA) for remote and long-term coastal ecosystem monitoring. *Sensors*, **11**(6):5850-5872. [doi:10.3390/s110605850]

Barnes, C.R., Tunnicliffe, V., 2008. Building the world's first multi-node cabled ocean observatories (NEPTUNE Canada and VENUS, Canada): science, realities, challenges and opportunities. Proc. OCEANS, p.1-8. [doi:10.1109/OCEANSKOBE.2008.4531076]

Cena, G., Bertolotti, I.C., Scanzio, S., *et al.*, 2012. Evaluation of EtherCAT distributed clock performance. *IEEE Trans. Ind. Inform.*, **8**(1):20-29. [doi:10.1109/TII.2011.2172434]

Chan, T., 2007. Analytical Methods for Power Monitoring and Control in an Underwater Observatory. PhD Thesis, University of Washington, USA.

Chave, A.D., Waterworth, G., Maffei, A.R., *et al.*, 2004. Cabled ocean observatory systems. *Mar. Technol. Soc. J.*, **38**(2):30-43. [doi:10.4031/002533204787522785]

Chen, Y.H., Yang, C.J., Li, D.J., *et al.*, 2012. Development of a direct current power system for a multi-node cabled ocean observatory system. *J. Zhejiang Univ.-Sci. C (Comput. & Electron.)*, **13**(8):613-623. [doi:10.1631/jzus.C1100381]

Chen, Y.H., Yang, C.J., Li, D.J., *et al.*, 2013. Study on 10 kV DC powered junction box for a cabled ocean observatory system. *China Ocean Eng.*, **27**(2):265-275. [doi:10.1007/s13344-013-0023-y]

del Río, J., Toma, D., Shariat-Panahi, S., *et al.*, 2012. Precision timing in ocean sensor systems. *Meas. Sci. Technol.*, **23**(2):025801.1-025801.7. [doi:10.1088/0957-0233/23/2/025801]

Dewey, R., Tunnicliffe, V., 2003. VENUS: future science on a coastal mid-depth observatory. Proc. 3rd Int. Workshop on Scientific Use of Submarine Cables and Related Technologies, p.232-233. [doi:10.1109/SSC.2003.1224149]

Han, J., Jeong, D., 2010. A practical implementation of IEEE 1588-2008 transparent clock for distributed measurement and control systems. *IEEE Trans. Instrument. Meas.*, **59**(2):433-439. [doi:10.1109/TIM.2009.2024371]

Howe, B.M., Chan, T., El-Sharkawi, M., *et al.*, 2006. Power System for the MARS Ocean Cabled Observatory. Available from http://neptunepower.apl.washington.edu/publications/documents/psftmoco.pdf [Accessed on Mar. 9, 2015].

Hsu, S.K., Lee, C.S., Shin, T.C., *et al.*, 2007. Marine cable hosted observatory (MACHO) project in Taiwan. Proc. Symp. on Underwater Technology and Workshop on Scientific Use of Submarine Cables and Related Technologies, p.305-307. [doi:10.1109/UT.2007.370808]

Ioannides, M.G., 2004. Design and implementation of PLC-based monitoring control system for induction motor. *IEEE Trans. Energy Conv.*, **19**(3):469-476. [doi:10.1109/TEC.2003.822303]

Kawaguchi, K., Kaneda, Y., Araki, E., 2008. The DONET: a real-time seafloor research infrastructure for the precise earthquake and tsunami monitoring. Proc. OCEANS, p.1-4. [doi:10.1109/OCEANSKOBE.2008.4530918]

Lentz, S., Lécroart, A., 2009. Precision timing in the NEPTUNE Canada network. Proc. OCEANS, p.1-5. [doi:10.1109/OCEANSE.2009.5278121]

Li, D.J., Wang, G., Yang, C.J., *et al.*, 2013. IEEE 1588 based time synchronization system for a seafloor observatory network. *J. Zhejiang Univ.-Sci. C (Comput. & Electron.)*, **14**(10):766-776. [doi:10.1631/jzus.C1300084]

Li, D.J., Wang, J., Zhang, Z.F., *et al.*, 2015. Research and implementation of an IEEE 1588 PTP-based time synchronization system for Chinese experimental ocean observatory network. *Mar. Technol. Soc. J.*, **49**(1):47-58. [doi:10.4031/MTSJ.49.1.10]

Lu, S., 2006. Infrastructure, Operations, and Circuits Design of an Undersea Power System. PhD Thesis, University of Washington, USA.

Milevsky, A., Walrod, J., 2008. Development and test of IEEE 1588 precision timing protocol for ocean observatory networks. Proc. OCEANS, p.1-7. [doi:10.1109/OCEANS.2008.5152029]

Ouellette, M., Ji, K., Liu, S., *et al.*, 2011. Using IEEE 1588 and boundary clocks for clock synchronization in telecom networks. *IEEE Commun. Mag.*, **49**(2):164-171. [doi:10.1109/MCOM.2011.5706325]

Pirenne, B., Guillemot, E., 2009. The data management system for the VENUS and NEPTUNE cabled observatories. Proc. OCEANS, p.1-4. [doi:10.1109/OCEANSE.2009.5278187]

Qi, J., Wang, L., Jia, H., *et al.*, 2010. Design and performance evaluation of networked data acquisition systems based on EtherCAT. Proc. 2nd IEEE Int. Conf. on Information Management and Engineering, p.467-469. [doi:10.1109/ICIME.2010.5478109]

Sun, T., Zhao, B., Li, F., 2011. Application of WinCC in carplant monitoring system. Proc. Int. Symp. on Computer Science and Society, p.203-205. [doi:10.1109/ISCCS.2011.63]

Woodroffe, A.M., Pridie, S.W., Druce, G., 2008. The NEPTUNE Canada junction box-interfacing science instruments to sub-sea cabled observatories. Proc. OCEANS, p.1-5. [doi:10.1109/OCEANSKOBE.2008.4531021]

Yu, Y., Xu, H., Jiang, E., 2011. The primary research of the junction box based seafloor observatory remote control system. Proc. Int. Conf. on Multimedia Technology, p.3750-3753. [doi:10.1109/ICMT.2011.6002721]